Geological Society of America
Special Paper 377
2004

Precambrian meta-ultramafic rocks from the Tobacco Root Mountains, Montana

Kathleen E. Johnson*
Department of Geology and Geophysics, University of New Orleans, New Orleans, Louisiana 70148, USA

John B. Brady
Department of Geology, Smith College, Northampton, Massachusetts 01063, USA

William A. MacFarlane
Colorado College, Colorado Springs, Colorado 80903, USA

Rebecca B. Thomas
Williams College, Williamstown, Massachusetts 01267, USA

Chris J. Poulsen
Carleton College, Northfield, Minnesota 55057, USA

M. Jennifer Sincock
Franklin & Marshall College, Lancaster, Pennsylvania 17604-3003, USA

ABSTRACT

Meta-ultramafic rocks occur as small (2 to 100 m long), podiform bodies in all three major Precambrian rock suites of the Tobacco Root Mountains of southwest Montana. Most samples consist of a randomly oriented, coarse-grained assemblage of orthopyroxene, olivine, and magnesiohornblende ± spinel, partially replaced by a fine-grained assemblage that may include anthophyllite, talc, cummingtonite, magnesiohornblende, chlorite, serpentine, and/or magnetite. Blackwall reaction zones of anthophyllite, actinolite, chlorite, and/or biotite surround several of the meta-ultramafic bodies. The absence of clinopyroxene with orthopyroxene limits the metamorphic pressure-temperature history of these rocks to temperatures below ~800 °C. The presence of anthophyllite with olivine indicates that these rocks passed through 650–700 °C at pressures below 0.6 GPa. These constraints are consistent with the detailed pressure-temperature path determined for the surrounding upper-amphibolite to granulite facies metamorphic rocks. Whole-rock chemical analyses of the meta-ultramafic rocks show them to be rich in SiO_2 (44–54 wt%) and poor in MgO (21–34 wt%) relative to mantle peridotites and typical Alpine-type ultramafic rocks. Rare earth element concentrations are all enriched relative to chondritic values and the light rare earth elements are especially enriched (10–30 times), inconsistent with either an upper-mantle or a komatiitic origin. All samples have similar TiO_2/Zr ratios, suggesting that they have a common or related origin, and that TiO_2 and Zr were conserved in the processes that led to the observed chemical variations. Together, the chemical data point to a protolith that was an ultramafic cumulate rich in orthopyroxene, and therefore probably formed in a continental setting from a basaltic magma enriched in silica. One possible time of origin is a magmatic event during the continental rifting at 2.06 Ga that led to the intrusion of a suite of mafic dikes.

Keywords: Big Sky orogeny, orthopyroxene, cumulate.

*Present address: P.O. Box 8352, Monterey, California 93940, USA, volcan@mac.com.

Johnson, K.E., Brady, J.B., MacFarlane, W.A., Thomas, R.B., Poulsen, C.J., and Sincock, M.J., 2004, Precambrian meta-ultramafic rocks from the Tobacco Root Mountains, Montana, *in* Brady, J.B., Burger, H.R., Cheney, J.T., and Harms, T.A., eds., Precambrian geology of the Tobacco Root Mountains, Montana: Boulder, Colorado, Geological Society of America Special Paper 377, p. 71–87.

INTRODUCTION

Lenses of deformed and metamorphosed ultramafic rocks occur within many Archean and Proterozoic supracrustal terranes (e.g., Paktunc, 1984; Srikantappa et al., 1984; Wilson and Hyndman, 1990; Occhipinti et al., 1998; Kalsbeek and Manatschal, 1999). The original character and origin of these meta-ultramafic rocks is largely obscured by the metamorphism to which they have been subjected, their tectonic disruption, and their isolation within more siliceous rocks. In some cases, relict grains from the original mineral assemblages suggest a parent material of mantle peridotite composition. In other cases, spinifex textures point to a komatiitic origin. Precambrian rocks of the Tobacco Root Mountains and the Ruby Range of the Wyoming province include a number of such ultramafic bodies (e.g., Merrill, 1895; Heinrich, 1963; Root, 1965; Burger, 1966, 1967; Hess, 1967; Gillmeister, 1972, 1976; Cordua, 1973; Hanley, 1975; Friberg, 1976; Tendall, 1978; Garihan, 1979; Desmarais, 1981; Cummings and McCulloch, 1992; MacFarlane, 1996a, 1996b; Thomas, 1996a, 1996b) whose tectonic and petrologic significance have been elusive.

A variety of hypotheses have been proposed for the origin of the meta-ultramafic pods in the Tobacco Root Mountains and adjacent Ruby Range. They have been interpreted as (1) forcibly emplaced hydrous peridotitic magmas (Heinrich, 1963); (2) "Alpine-type ultramafic intrusives" (Cordua, 1973); (3) "cumulates of a differentiating basaltic magma" emplaced in the solid state (Tendall, 1978); (4) tectonically emplaced, cold ultramafic bodies that were serpentinized prior to metamorphism (Desmarais, 1981); (5) "a sliver of oceanic crust generated during ensialic basin development" (Cummings and McCulloch, 1992); and (6) metamorphosed komatiite lavas or intrusions (MacFarlane, 1996b; Johnson et al., 1996). In this paper we present new geochemical and mineralogic data that place important constraints on the origin and history of the Tobacco Root meta-ultramafic rocks. We use these new data to argue for an igneous cumulate origin and, therefore, tectonic emplacement of these rocks, similar to the preferred interpretation of Tendall (1978) based on modal data.

FIELD RELATIONS

Meta-ultramafic rocks of the Tobacco Root Mountains occur as small bodies (2–100 m across), typically with lens-shaped map patterns, hosted by three distinct units: (1) the Spuhler Peak Metamorphic Suite—a mafic unit that consists principally of amphibolite and Ca-depleted amphibolite, with lesser quartzite and aluminous schist; (2) the Indian Creek Metamorphic Suite—quartzofeldspathic gneiss and amphibolite interlayered with many rocks that are clearly metasediments, including quartzite, marble, iron formation, and aluminous schist; and (3) the Pony–Middle Mountain Metamorphic Suite—principally quartzofeldspathic gneiss and hornblende amphibolite (see Burger, 2004, this volume, Chapter 1). Although all three suites contain meta-ultramafic pods, a significant portion of the bodies occurs within the Spuhler Peak Metamorphic Suite (Fig. 1). A number of the meta-ultramafic bodies, particularly those well exposed in the high-elevation Branham Lakes area, are flattened subparallel to the surrounding foliation. Other meta-ultramafic bodies are more equant in form and have contacts that make a high angle to the surrounding foliation. In many cases, the contacts are not exposed, as if the contact were a site of enhanced weathering. Most bodies are unfoliated and show little evidence of internal deformation. Where present, foliation tends to be parallel to that in the surrounding gneisses. Most meta-ultramafic rocks within the Indian Creek and Pony–Middle Mountain Metamorphic Suites occur at lower elevations as tree-covered hills surrounded by low-lying felsic gneisses that support only grass. Here the structural relations are obscure because outcrop is poor and ultramafic rock–gneiss contacts are not exposed. Additional field data concerning the meta-ultramafic rocks can be found in a number of theses on the Tobacco Root Mountains (Root, 1965; Burger, 1966, 1967; Hess, 1967; Gillmeister, 1972; Cordua, 1973; Hanley, 1975; Friberg, 1976; Tendall, 1978; Poulsen, 1994; Sincock, 1994; MacFarlane, 1996b; Thomas, 1996b).

Most Tobacco Root meta-ultramafic rocks have a coarse texture with prominent prismatic crystals. Randomly oriented, dark green amphibole blades 1–3 cm long highlight many samples. Where more weathered, the amphibole grains have a silvery cast and are set in a rusty matrix. A few outcrops contain large (3–6 cm), tan orthopyroxene crystals (Fig. 2) that resist weathering to form a knobby texture. An outcrop on the ridge west of Branham Lakes exhibits an unusual texture of radiating amphibole sprays up to 3 cm across and is cut by a small pegmatite. Serpentine partially replaces olivine and orthopyroxene in many bodies. The largest ultramafic body (>100 m across), which forms a tree-covered knob at the end of Granite Creek Road in the southern Tobacco Root Mountains, has a core of relatively fresh peridotite surrounded by a zone of serpentinite. Several meta-ultramafic bodies have "blackwall" reaction zones (see Sanford, 1982) along contacts with the enclosing gneisses or amphibolites. Blackwall sequences up to 0.5 m in width consist principally of anthophyllite, actinolite, chlorite, and/or biotite, commonly in near monomineralic bands. The chlorite and biotite reaction zones are typically foliated parallel to the contact. Folds were observed in a chloritic blackwall in Beuler Cirque.

Many ultramafic bodies in orogenic belts have been tectonically emplaced, and that is our interpretation for the Tobacco Root meta-ultramafic bodies (see below). This means that they are surrounded by faults. However, we have not been able to trace the faults because of the extensive deformation associated with the Big Sky orogeny that rotated and obscured many primary structures (Harms et al., 2004, this volume, Chapter 10). However, even if they were originally komatiitic lava flows or intrusions, or had another origin, their present form and distribution indicate that the meta-ultramafic units have been tectonically disrupted, as if they were stiff bodies in a more ductile matrix. Cummings and McCulloch (1992) observed that the Branham Lakes meta-ultramafic rocks are associated with shear zones

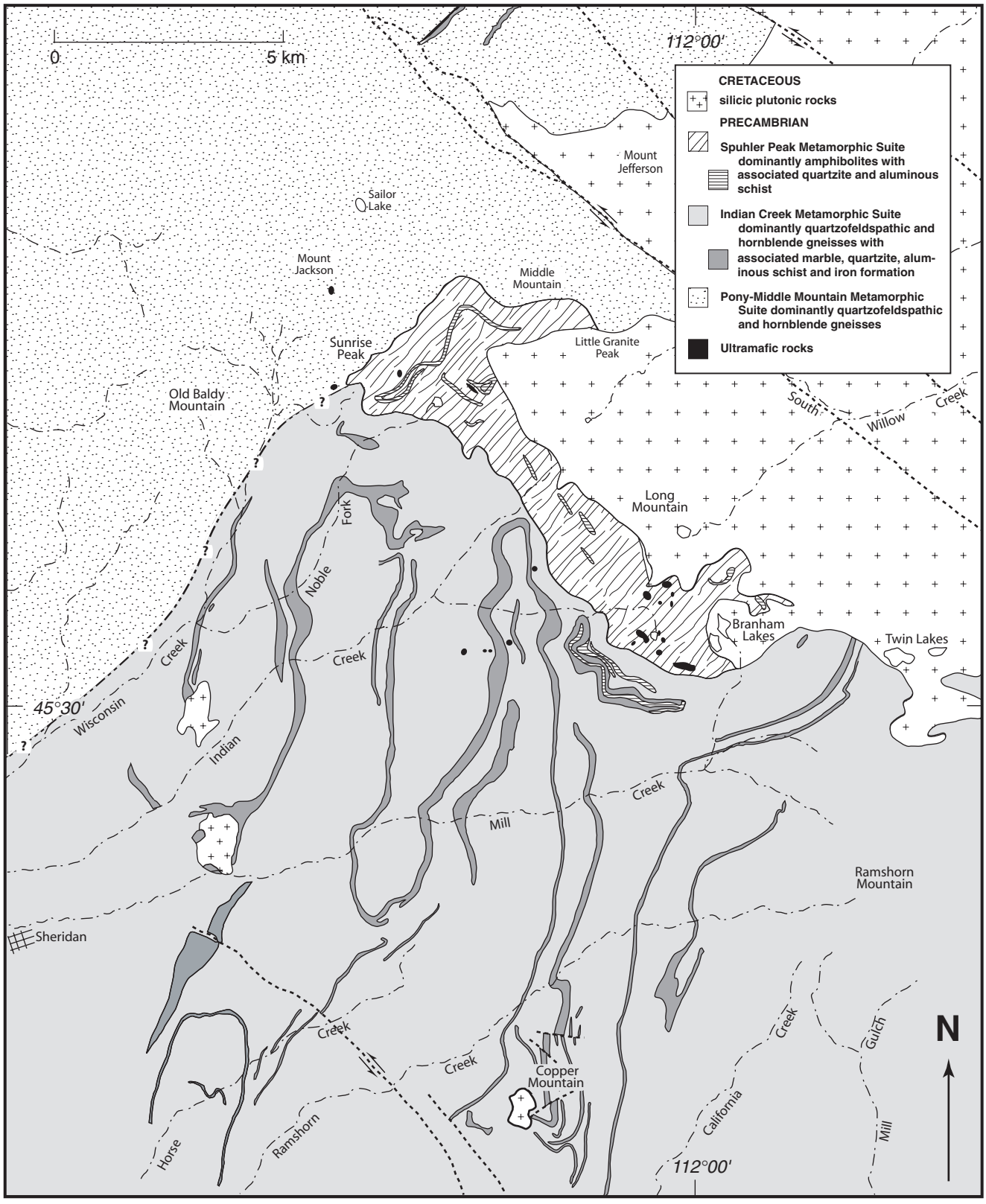

Figure 1. Geologic map of the central portion of the Tobacco Root Mountains, modified from Vitaliano et al. (1979). Meta-ultramafic bodies in and around the Spuhler Peak Metamorphic Suite are shown in black. Additional meta-ultramafic bodies in the northern and southern parts of the range are displayed on the original Vitaliano et al. (1979) map (see reprinted map and text accompanying this volume).

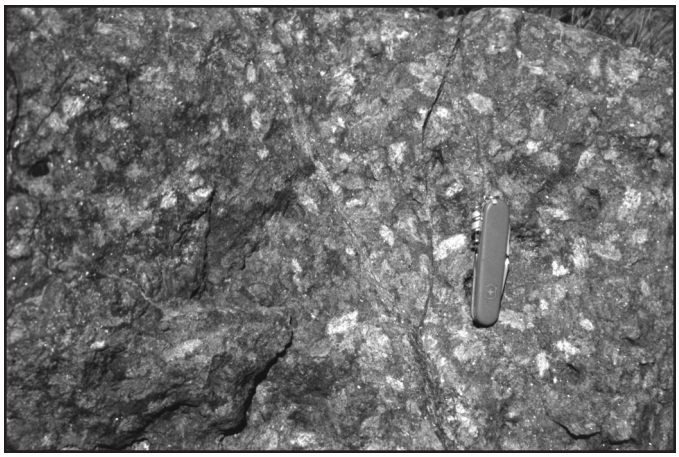

Figure 2. An outcrop of meta-ultramafic rock near Branham Lakes showing elongated, tan, weathered, orthopyroxene crystals in a matrix of gray green magnesiohornblende. The pocketknife in the photo is 8.5 cm long.

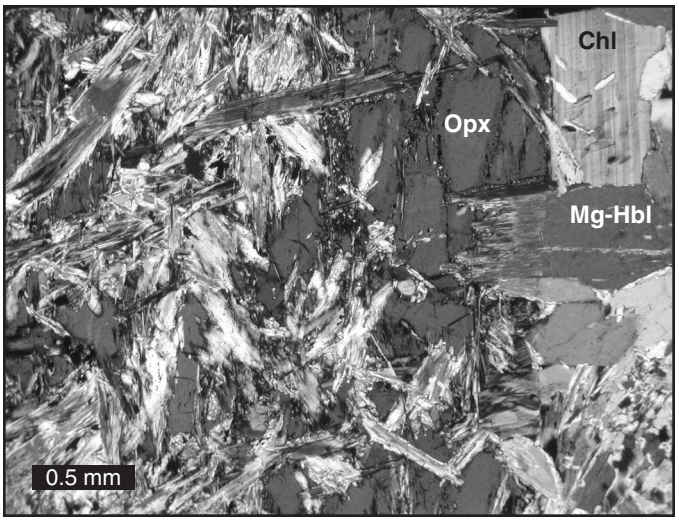

Figure 3. Photomicrograph in cross-polarized light of a Spuhler Peak Metamorphic Suite–hosted meta-ultramafic rock that contains large (>1 cm) grains of orthopyroxene. The left part of the field of view consists of the amphiboles magnesiohornblende (darker) and anthophyllite (lighter). They are replacing a large orthopyroxene (Opx) crystal. Many magnesiohornblende (Mg-Hbl) crystals are zoned and have tremolite rims. Chlorite (Chl) is also visible. Sample JBB-93-2 from west of Branham Lakes.

within the Spuhler Peak Metamorphic Suite. Similar structural characteristics were observed by Desmarais (1981) for the meta-ultramafic pods of the adjacent Ruby Range, which we believe experienced a metamorphic history similar to the Tobacco Root Mountains. He described boudin-shaped bodies that are concordant with respect to deformational structures of the host gneisses, and that most commonly occur within zones of intense plastic deformation. In cases where there is structural discordance between meta-ultramafic rocks and host gneisses, Desmarais (1981) suggested tectonic emplacement within the noses of isoclinal folds. The occurrence of ultramafic pods within fold hinges or as apparent boudins within shear zones is a common feature in other Precambrian terranes (e.g., Paktunc, 1984; Srikantappa et al., 1984; Jahn and Zhang, 1984; Occhipinti et al., 1998; Rosing and Rose, 1993; Kalsbeek and Manatschal, 1999).

PETROGRAPHY

In thin section the meta-ultramafic rocks typically display complex textures, with fine-grained, generally hydrous minerals such as magnesiohornblende, tremolite, anthophyllite, magnesiocummingtonite, talc, chlorite, phlogopite, and serpentine overgrowing and/or replacing coarse orthopyroxene, olivine, and magnesiohornblende. Spinel and magnetite are minor constituents of most samples. Figure 3 shows a typical texture in cross-polarized light. Much of the field of view in Figure 3 is filled with part of a cm-sized orthopyroxene crystal (dark gray) covered by randomly oriented elongate or fibrous amphiboles. Many of the light-colored amphiboles are anthophyllite, whereas the darker ones in this cross-polarized image are calcic amphiboles that are rich in magnesium (magnesiohornblende; see Table 1). Most of the minerals are colorless or very pale, reflecting low iron contents. Pale green magnesiohornblende grains typically have color and interference-color bands, reflecting their chemical zonation from magnesiohornblende (core) toward tremolite (rim). Figure 4 shows a simpler texture, in plane-polarized light, consisting of rounded, light-colored olivine crystals set among magnesiohornblende crystals of various sizes. This appears to be an equilibrium texture, not a replacement of high-grade minerals during cooling.

Textures of the meta-ultramafic rocks possess features in common with metamorphic rocks of other compositions that surround them in the Tobacco Root Mountains (see Cheney et al., 2004a, this volume, Chapter 6). Remnants of a coarse-textured, high-*P*-*T* (pressure-temperature) mineral assemblage are overgrown by finer-grained minerals produced during decompression and cooling. Based on grain size, the high-*P*-*T* assemblage would have been principally orthopyroxene, olivine, magnesiohornblende, and spinel. We found no evidence of clinopyroxene or garnet in this assemblage; nor were these minerals found in the adjacent Ruby Range by Desmarais (1981). However, a few occurrences of clinopyroxene or garnet have been reported by others for the Tobacco Root Mountains (see next section). Anthophyllite is common among the fine-grained minerals; talc is less abundant. Serpentine is not particularly abundant, except in a few ultramafic bodies. Evidence of deformation of orthopyroxene and olivine in the meta-ultramafic samples is limited, with most fabric, if present, defined by amphiboles. This contrasts with Alpine-type peridotites that retain features of intracrystalline deformation induced during emplacement. We think that the absence of deformation textures is evidence that these rocks were completely recrystallized during metamorphism of the Tobacco Root terrane.

TABLE 1. CHEMICAL COMPOSITIONS OF MINERALS IN META-ULTRAMAFIC ROCKS

Sample	KEJ-20	KEJ-20	KEJ-20	KEJ-20	KEJ-20	KEJ-20	KEJ-20	KEJ-20	TBR-68b	TBR-68b	TBR-68b
Host	SPMS	SPMS	SPMS	SPMS	SPMS	SPMS	SPMS	SPMS	SPMS	SPMS	SPMS
12T	042123E	042123E	042123E	042123E	042123E	042123E	042123E	042123E	042125E	042125E	042125E
UTM	504063N	504063N	504063N	504063N	504063N	504063N	504063N	504063N	504058N	504058N	504058N
Mineral	Ol	Ol	Opx	Opx	Ant	Ant	Tr	Chl	Opx	Ant	Mg-Hbl
Oxide wt%											
SiO_2	39.64	39.65	55.72	53.70	55.96	58.52	58.70	32.02	54.14	59.93	51.44
Al_2O_3	0.03	0.00	0.86	0.79	0.41	0.51	0.12	15.93	2.93	0.09	7.00
TiO_2	0.00	0.05	0.02	0.00	0.07	0.02	0.04	0.03	0.07	0.00	0.32
MgO	42.63	42.30	30.99	31.57	28.41	27.38	23.46	31.71	28.74	27.04	20.20
*FeO	17.77	17.82	12.15	12.68	11.79	10.79	3.88	6.05	12.34	9.88	6.29
MnO	0.70	0.79	0.76	0.84	0.96	0.96	0.43	0.12	0.68	0.91	0.43
CaO	0.00	0.04	0.20	0.20	0.30	0.43	11.42	0.00	0.22	0.53	10.59
Na_2O	0.14	0.18	0.21	0.14	0.08	0.28	0.12	0.11	0.19	0.29	1.06
K_2O	0.00	0.00	0.00	0.00	0.01	0.00	0.00	0.00	0.00	0.00	0.06
Total	100.92	100.83	100.91	99.91	98.00	98.90	98.17	85.97	99.32	98.68	97.39
Elements per Formula											
O	4	4	6	6	23	23	23	7	6	23	23
Si	1.00	1.00	1.96	1.92	7.74	7.95	8.01	1.55	1.94	8.10	7.21
Al	0.00	0.00	0.04	0.03	0.07	0.08	0.02	0.91	0.12	0.02	1.16
Ti	0.00	0.00	0.00	0.00	0.01	0.00	0.00	0.00	0.00	0.00	0.03
Mg	1.60	1.60	1.63	1.69	5.86	5.54	4.77	2.29	1.53	5.45	4.22
Fe	0.38	0.38	0.36	0.38	1.36	1.23	0.44	0.24	0.37	1.12	0.74
Mn	0.02	0.02	0.02	0.03	0.11	0.11	0.05	0.00	0.02	0.10	0.05
Ca	0.00	0.00	0.01	0.01	0.04	0.06	1.67	0.00	0.01	0.08	1.59
Na	0.01	0.01	0.01	0.01	0.02	0.07	0.03	0.01	0.01	0.08	0.29
K	0.00	0.00	0.00	0.01	0.00	0.00	0.00	0.00	0.00	0.00	0.01
Total Cations	3.00	3.00	4.02	4.07	15.22	15.05	15.00	5.00	4.01	14.93	15.30
Mg/(Mg+Fe)	0.81	0.81	0.82	0.82	0.81	0.82	0.92	0.90	0.81	0.83	0.85

(continued)

Chemical compositions of representative minerals from meta-ultramafic samples hosted by each of the three metamorphic suites are listed in Table 1. These data were collected at Amherst College using a Link/Oxford energy-dispersive X-ray spectrometer and mineral standards. Olivine compositions are typically $Fo_{81–83}$ with associated orthopyroxene compositions slightly more magnesian ($En_{82–84}$). Amphiboles are also magnesium-rich with anthophyllite closely matching the Mg/(Mg + Fe) value (X_{Mg}) of adjacent olivine; magnesiohornblende has a higher X_{Mg} value, and tremolite is even more magnesian ($X_{Mg} \geq 0.90$). Where present, green chromian spinels have X_{Mg} of 0.41–0.55 and Cr/(Cr + Al) of 0.29–0.08. Most chlorites have low Al and a high X_{Mg} (≥0.90). The data in Table 1 are quite similar to mineral analyses reported by Tendall (1978) for the Tobacco Root Mountains and Desmarais (1981) for the Ruby Range.

METAMORPHISM

The observed coarse-grained mineral assemblage of orthopyroxene, olivine, and magnesiohornblende and the absence of clinopyroxene in our samples places an important constraint on the *P-T* path of these rocks. The "clinopyroxene-in" reaction

$$Fo + Tr = Di + En + H_2O$$

for the Mg-rich portion of the CaO-MgO-SiO_2-H_2O (CMSH) system is shown in Figure 5 (reaction 3), as calculated by Spear (1993) from the Berman (1988) thermodynamic database. Also shown in Figure 5 (dashed line at slightly higher temperature) is a CMSH version of this reaction calculated by Schmädicke (2000, Figure 12 therein) using the Holland and Powell (1998) database (1993 version). In either case, the maximum temperature during the high-pressure stage (≥1.0 GPa) is limited to ~800 °C by the absence of clinopyroxene with orthopyroxene.

Another constraint on the *P-T* path is given by the presence of post-peak anthophyllite. The bulk compositions determined for the Tobacco Root meta-ultramafic rocks (see next section) are shown in Figure 5 as black triangles on a composition diagram of the system diopside ($Ca_2Mg_2Si_4O_{12}$), quartz (Si_6O_{12}), forsterite ($Mg_6Si_3O_{12}$). Because most of the iron in the rocks is contained in the minerals on this diagram, FeO was added to MgO in calculating the plotting positions of the bulk compositions. An average value of these compositions is shown with an "X" on the other ternary phase assemblage diagrams to indicate the expected mineral assemblages. As is evident from Figure 5, anthophyllite

TABLE 1. CHEMICAL COMPOSITIONS OF MINERALS IN META-ULTRAMAFIC ROCKS (*continued*)

Sample	RBT-28	RBT-28	RBT-28	RBT-28	RBT-28	TBR-84	TBR-85	TBR-86	TBR-87	TBR-88	TBR-89
Host	PMMMS	PMMMS	PMMMS	PMMMS	PMMMS	ICMS	ICMS	ICMS	ICMS	ICMS	ICMS
12T	042803E	042803E	042803E	042803E	042803E	041663E	041663E	041663E	041663E	041663E	041663E
UTM	506327N	506327N	506327N	506327N	506327N	504011N	504011N	504011N	504011N	504011N	504011N
Mineral	Ol	Opx	Spl	Mg-Hbl	Chl	Opx	Spl	Spl	Mg-Hbl	Mg-Hbl	Chl
Oxide wt%											
SiO_2	39.51	55.97	0.11	51.70	42.12	55.20	0.21	0.14	52.99	52.70	50.40
Al_2O_3	0.06	2.28	53.87	6.12	0.76	1.90	53.75	52.25	5.90	7.03	4.00
TiO_2	0.00	0.17	0.05	0.58	0.02	0.07	0.08	0.05	0.35	0.57	0.07
MgO	43.29	31.15	14.66	19.98	30.66	29.61	13.11	12.04	20.25	19.96	31.52
*FeO	15.86	10.87	21.97	4.85	8.93	12.03	20.85	22.47	5.01	4.55	4.42
MnO	0.43	0.42	0.30	0.19	0.74	0.22	0.10	0.14	0.08	0.07	0.05
CaO	0.02	0.21	0.00	12.50	0.37	0.35	0.07	0.01	11.89	12.56	0.05
Na_2O	0.27	0.24	0.53	0.54	0.30	0.00	0.19	0.25	0.39	0.69	0.14
K_2O	0.00	0.00	0.02	0.20	0.03	0.00	0.00	0.00	0.12	0.09	0.07
Cr_2O_3	N.D.	N.D.	7.37	0.45	0.00	0.20	9.96	10.23	0.66	0.35	0.13
Total	99.44	101.32	98.88	97.12	83.93	99.58	98.32	97.58	97.65	98.57	90.85
Elements per Formula											
O	4	6	4	23	7	6	4	4	23	23	7
Si	1.00	1.95	0.00	7.26	2.10	1.96	0.01	0.00	7.37	7.27	2.22
Al	0.00	0.09	1.75	1.01	0.04	0.08	1.75	1.73	0.97	1.14	0.21
Ti	0.00	0.00	0.00	0.06	0.00	0.00	0.00	0.00	0.04	0.06	0.00
Mg	1.64	1.61	0.60	4.18	2.28	1.57	0.54	0.51	4.20	4.10	2.07
Fe	0.34	0.32	0.51	0.57	0.37	0.36	0.48	0.53	0.58	0.53	0.16
Mn	0.01	0.01	0.01	0.02	0.03	0.01	0.00	0.00	0.01	0.01	0.00
Ca	0.00	0.01	0.00	1.88	0.02	0.01	0.00	0.00	1.77	1.86	0.00
Na	0.01	0.02	0.03	0.15	0.03	0.00	0.01	0.01	0.11	0.18	0.01
K	0.00	0.00	0.00	0.04	0.00	0.00	0.00	0.00	0.02	0.02	0.00
Cr	N.D.	N.D.	0.16	0.05	0.00	0.01	0.22	0.23	0.07	0.04	0.00
Total Cations	3.00	4.01	3.05	15.23	4.89	4.00	3.01	3.02	15.14	15.20	4.68
Mg/(Mg+Fe)	0.83	0.84	0.54	0.88	0.86	0.81	0.53	0.49	0.88	0.89	0.93

Note: Data from Thomas (1996b). SPMS—Spuhler Peak Metamorphic Suite; PMMMS—Pony–Middle Mountain Metamorphic Suite; ICMS—Indian Creek Metamorphic Suite; Ol—olivine; Opx—orthopyroxene; Ant—anthophyllite; Tr—tremolite; Chl—chlorite; Mg-Hbl—magnesiohornblende.

*FeO—total iron as FeO

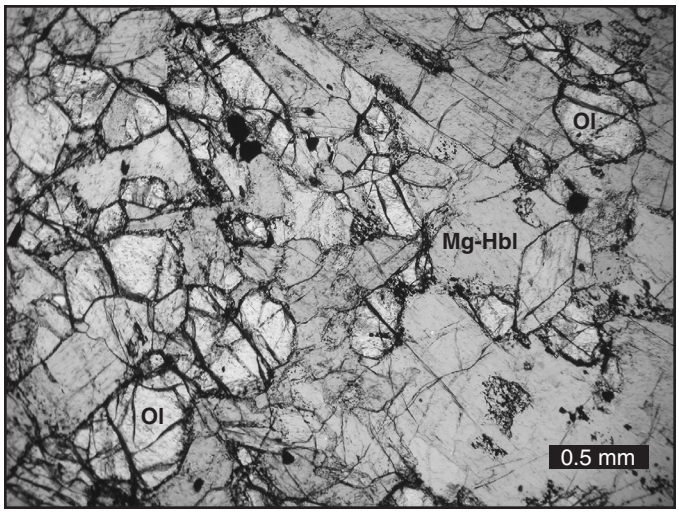

Figure 4. Photomicrograph in plane-polarized light of a Spuhler Peak Metamorphic Suite–hosted meta-ultramafic rock that contains rounded olivine (Ol) crystals in a matrix of coarse magnesiohornblende (Mg-Hbl). The grain boundaries and fractures are dusted with small crystals of magnetite and perhaps other oxide minerals. Sample RBT-22 collected west of Branham Lakes.

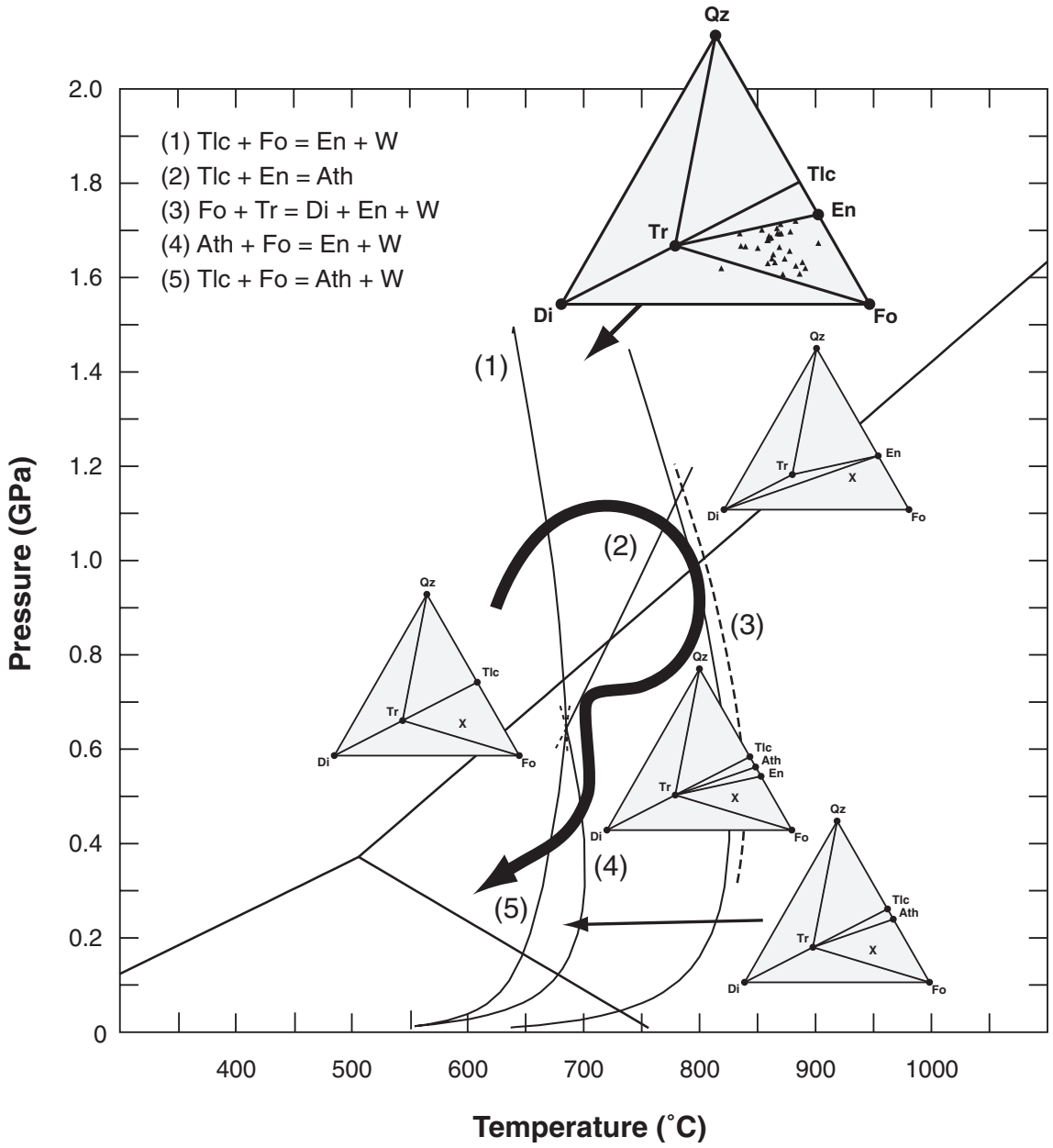

Figure 5. Pressure-temperature diagram showing selected end-member chemical reactions for ultramafic rocks during metamorphism. Minerals involved are quartz (Qz), forsterite (Fo), diopside (Di), tremolite (Tr), enstatite (En), talc (Tlc), anthophyllite (Ath), and water (W). Locations of the reactions were calculated by Spear (1993) for $P_{H_2O} = P_{total}$ using the thermodynamic database of Berman (1988). Mineral assemblages are shown on a composition diagram in oxygen units with $Ca_2Mg_2Si_4O_{12}$ (Di), Si_6O_{12} (Qz), and $Mg_6Si_3O_{12}$ (Fo) at the corners. Bulk compositions of Tobacco Root meta-ultramafic rocks (Table 2) are shown on one diagram and are represented by an X on other diagrams (see text). The *P-T* path shown by the dark arrow is proposed for the Tobacco Root Mountains based on the petrology of other rock types (Cheney et al., 2004a, this volume, Chapter 6). The absence of clinopyroxene with orthopyroxene in the meta-ultramafic rocks indicates that the *P-T* path passes to the left of reaction 3. The presence of anthophyllite is consistent with a *P-T* path that includes temperatures between 650 and 700 °C at pressures below 0.6 GPa.

+ olivine stably coexist in rocks with the "X" bulk composition only at pressures below ~0.6 GPa and at temperatures between 650 and 700 °C. We conclude, therefore, that the meta-ultramafic rocks passed through these conditions during cooling.

The Precambrian rocks of the Tobacco Root Mountains have been metamorphosed twice and contain mineral assemblages reflecting upper-amphibolite to granulite facies conditions (Reid, 1963). Cheney et al. (2004b, this volume, Chapter 8) and Mueller et al. (2004, this volume, Chapter 9) demonstrate that these metamorphic events occurred at 2.45 Ga and 1.78–1.72 Ga. Cheney et al. (2004a, this volume, Chapter 6) propose a *P-T* path for the 1.78–1.72 metamorphism (the Big Sky orogeny), which is reproduced in Figure 5 as a heavy black line. The clockwise *P-T* path is based in part on the superposition of fine-grained, 700 °C, 0.6–0.8 GPa mineral assemblages (e.g., garnet + cordierite) on coarse-grained, 750 °C, 1.0 GPa mineral assemblages (e.g., kyanite + orthopyroxene). The unusual "kink" in the *P-T* path is based on the occurrence of garnet necklaces surrounding orthopyroxene in a plagioclase-rich rock (produced by near isobaric cooling) and the nearby occurrence of orthopyroxene + plagioclase pseudomorphs after garnet in a hornblende-rich rock (produced by near isothermal decompression). See Cheney et al. (2004a, this volume, Chapter 6) for details. Interestingly, this independently determined path is consistent with the two principal constraints provided by the meta-ultramafic rocks.

Hess (1967), Cordua (1973), Tendall (1978), and Wilson and Hyndman (1990) all reported diopside as a minor phase in meta-ultramafic rocks containing orthopyroxene. This could be due to higher metamorphic temperatures, but we think it is more likely due to locally lower values of a_{H_2O}. Gillmeister (1976) reported garnet ($Py_{40}Alm_{40}Gr_{17}Sp_3$) in a more iron-rich ultramafic rock consisting of orthopyroxene (En_{76}), olivine (Fo_{74}), and magnesiohornblende from the central Tobacco Roots. Cordua (1973) and Tendall (1978) also reported garnet. We did not observe garnet in any meta-ultramafic sample, so we suspect that the presence of garnet is due to a more iron-rich bulk composition.

WHOLE-ROCK GEOCHEMISTRY

Analytical Methods

Large samples were collected in the field with the goal of obtaining representative whole-rock chemical analyses. Two to three fist-sized or larger samples were collected from each location to ensure that the sample would be at least 20 times the size of the largest crystal or pseudomorph after all weathered portions were removed. Samples were prepared and analyzed for major and trace elements by X-ray fluorescence spectroscopy following standard procedures at Franklin and Marshall College (Sincock, 1994), Carleton College (Poulsen, 1994), or Colorado College (MacFarlane, 1996b). Rare earth element (REE) and other trace element analyses of a subset of the samples were determined by neutron activation analysis at Oregon State University under the Department of Energy–sponsored Reactor Sharing Program (http://ne.oregonstate.edu/facilities/radiation_center/naa2.html) or by inductively coupled plasma–mass spectrometry at SGS Geochemical Exploration and Research Analysis Laboratories (formerly XRAL) in Toronto (http://www.sgs.ca/geochem/index.html).

Results

Chemical analyses for 32 meta-ultramafic samples are listed in Table 2. A wide range of major and trace element concentrations is evident, with some varying by a factor of two or more. The SiO_2 content (44–54 wt%) and MgO content (21–34 wt%) of these rocks (see Fig. 6) suggests a pyroxene-rich protolith, rather than a more olivine- or hornblende-rich protolith that would have ultrabasic chemistry (Wyllie, 1967). Mg numbers (molar Mg/(Mg + Fe) values times 100) are 74 to 84. Al_2O_3 varies from 4 to 10 wt% and CaO varies from 1 to 8 wt%, with CaO/Al_2O_3 (weight percent ratio) below one for most samples (Fig. 7). Based on normative calculations, an igneous rock protolith for these meta-ultramafic samples may have consisted primarily of orthopyroxene and olivine, with subordinate clinopyroxene and plagioclase (Fig. 8; Table 2). Total alkalis account for <1 wt%. Ni (500–1400 ppm) and to some extent Cr (1900–4900 ppm) concentrations are low relative to typical mantle peridotites (Hess, 1989, p. 86). For samples with REE analyses, all are enriched relative to chondritic values (Sun and McDonough, 1989), with most light rare earth elements (LREEs) 10–30 times chondritic values and heavy REEs 2–10 times chondritic values (Fig. 9). Several Spuhler Peak Metamorphic Suite–hosted ultramafic samples and one Indian Creek Metamorphic Suite–hosted sample exhibit negative Eu anomalies. Relative to a primitive mantle composition, these rocks are enriched in a variety of trace elements by 2 to 30 times (Fig. 10), whereas several samples are depleted in K, Sr, or Eu and all are enriched in Cs. Our data are consistent with ten analyses of meta-ultramafic rocks from the Branham Lakes area of the Tobacco Root Mountains reported by Cummings and McCulloch (1992) and more than span the range of their results.

Interpretation of the Geochemical Data

Because of the Precambrian age of the metamorphism of the Tobacco Root Mountains and the MgO contents (21–34 wt%) of the meta-ultramafic rocks, we looked for evidence that their protoliths may have been komatiitic magmas. The bulk chemical compositions straddle the boundary between ultramafic komatiites and basaltic komatiites on a Jensen (1976) cation plot (Fig. 11), as well as on other discriminant diagrams. Although no spinifex textures were observed, it is possible that they may have been destroyed during the granulite facies metamorphism experienced by these rocks. However, several other features of these rocks are not consistent with a komatiitic origin. Chondrite-normalized REE patterns for komatiites are typically LREE depleted (e.g., Arndt et al., 1977; Arndt and Nisbet, 1982), whereas the Tobacco Root rocks are LREE enriched. Crystal fractionation in komatiites is dominated by olivine, whereas the chemical

TABLE 2. WHOLE-ROCK CHEMICAL ANALYSES OF META-ULTRAMAFIC ROCKS

Host	SPMS	SPMS	SPMS	ICMS	ICMS	ICMS	PMMMS	PMMMS	PMMMS
12T	042126E	042148E	041704E	041722E	041729E	041839E	041426E	042392E	042803E
UTM	504059N	504148N	504553N	504014N	504015N	504203N	504841N	506541N	506327N
Sample	WAM-2b	WAM-6a	WAM-22b	WAM-18a	WAM-20b	WAM-31	WAM-8a	WAM-9b	WAM-13a
Oxide (wt%)									
SiO_2	51.02	47.94	52.83	52.93	51.56	48.09	50.45	49.60	46.80
TiO_2	0.29	0.36	0.34	0.37	0.39	0.27	0.39	0.26	0.24
Al_2O_3	6.54	6.72	5.63	5.42	7.84	6.69	5.09	5.12	5.09
*FeO	8.59	11.19	10.18	12.07	10.26	8.45	11.85	12.63	11.20
MnO	0.54	0.37	0.12	0.16	0.17	0.18	0.25	0.31	0.27
MgO	27.60	29.42	24.88	26.79	21.80	25.20	22.92	27.51	32.85
CaO	5.15	3.82	5.13	2.10	6.83	9.74	7.34	4.51	3.38
Na_2O	0.19	0.14	0.77	0.06	0.98	0.80	1.26	0.04	0.15
K_2O	0.03	0.00	0.07	0.06	0.11	0.50	0.39	0.00	0.00
P_2O_5	0.04	0.04	0.04	0.04	0.05	0.08	0.06	0.03	0.03
Total	100.00	100.00	100.00	100.00	100.00	100.00	100.00	100.00	100.00
Trace Elements (ppm)									
Sc	18.3	17.4	20.4	17.0	21.7	29.1	17.7	24.1	14.8
V	86	126	121	142	154	118	106	122	77
Cr	2020	2850	3309	3304	2140	2935	2038	2363	3561
Co	104	102	126	153	102	88	111	118	128
Ni	771	1180	1320	1270	702	840	918	670	1150
Zn	62	95	72	77	58	66	70	72	71
Rb	4	4	2	4	2	19	11	3	5
Sr	13	17	21	12	6	35	120	38	22
Y	8	11	15	10	11	12	15	8	9
Zr	36	48	39	49	48	33	51	29	33
Nb	6	4	7	4	4	3	5	3	1
Cs	N.D.[†]	0.55	0.52	0.45	N.D.	3.00	1.32	0.54	N.D.
La	3.7	8.7	4.1	7.9	7.3	10.1	7.7	2.9	5.7
Ce	9.0	19.9	10.5	15.4	15.5	23.7	19.3	6.5	12.4
Nd	4.1	8.0	5.9	7.2	8.1	12.8	10.8	3.5	5.9
Sm	0.90	1.33	1.16	1.49	1.39	2.48	2.06	0.63	0.86
Eu	0.13	0.26	0.18	0.13	0.44	0.64	0.60	0.20	0.28
Tb	0.14	0.18	0.24	0.26	0.25	0.29	0.30	0.14	0.14
Yb	0.68	0.81	0.99	1.18	1.04	0.92	0.97	0.59	0.58
Lu	0.10	0.10	0.16	0.21	0.17	0.09	0.15	0.10	0.08
Hf	0.89	1.19	0.96	1.73	1.41	1.01	1.38	0.58	0.70
Ta	0.12	0.22	0.17	0.15	0.17	0.09	0.16	0.06	0.08
Th	1.45	2.50	1.21	2.50	2.30	2.49	1.55	1.06	1.66
CIPW Weight Norms									
Or	0.2	0.0	0.4	0.4	0.7	3.0	2.3	0.0	0.0
Ab	1.6	1.2	6.5	0.5	8.3	6.8	10.7	0.3	1.3
An	16.9	17.7	11.7	10.2	16.7	13.2	7.1	13.8	13.2
C	0.0	0.0	0.0	1.5	0.0	0.0	0.0	0.0	0.0
Di	6.7	0.8	10.8	0.0	13.5	27.6	23.3	6.7	2.7
Hy	54.3	44.2	56.3	81.8	43.8	8.2	25.8	52.9	34.9
Ol	19.7	35.4	13.5	4.9	16.2	40.7	30.1	25.7	47.4
Il	1.0	1.0	1.0	1.0	1.0	1.0	1.0	0.0	0.0
Ap	0.0	0.0	0.0	0.0	0.0	0.0	0.0	0.0	0.0

(continued)

TABLE 2. WHOLE-ROCK CHEMICAL ANALYSES OF META-ULTRAMAFIC ROCKS (*continued*)

Host	SPMS	SPMS	SPMS	SPMS	SPMS	SPMS	SPMS	SPMS	SPMS	SPMS	SPMS	SPMS
12T	042133E	042073E	042080E	042075E	041546E	041547E	041493E	042125E	042123E	042089E	042120E	042141E
UTM	504171N	504063N	504057N	504064N	504658N	504660N	504591N	504058N	504063N	504049N	504139N	504138N
Sample	CP-16	CP-23	CP-29	CP-30	CP-54	CP-55	CP-58	WAM-2d	WAM-2e	WAM-3c	WAM-5a	WAM-6c
Oxide (wt%)												
SiO_2	44.90	50.93	45.77	49.59	51.22	52.57	48.21	50.52	45.68	47.97	50.68	51.18
TiO_2	0.25	0.27	0.24	0.21	0.33	0.29	0.30	0.29	0.25	0.36	0.36	0.25
Al_2O_3	5.70	5.57	4.54	4.58	5.82	4.26	5.62	6.86	4.82	6.90	6.83	6.63
FeO*	10.65	12.18	11.14	12.06	9.12	9.41	10.15	10.58	11.46	10.80	10.66	10.31
MnO	0.37	0.52	0.39	0.27	0.12	0.15	0.15	0.51	0.41	0.44	0.49	0.40
MgO	31.48	25.49	34.27	32.62	27.28	28.44	30.55	26.14	33.55	28.08	25.54	28.18
CaO	5.31	4.01	4.14	1.30	4.89	4.00	5.59	4.67	3.39	5.20	4.77	2.96
Na_2O	0.30	0.48	0.14	0.03	0.69	0.43	0.16	0.34	0.07	0.12	0.56	0.07
K_2O	0.09	0.09	0.05	0.04	0.20	0.09	0.05	0.06	0.33	0.05	0.05	0.00
P_2O_5	0.03	0.02	0.02	0.08	0.06	0.06	0.02	0.04	0.04	0.07	0.05	0.03
Total	99.08	99.57	100.69	100.79	99.74	99.72	100.80	100.00	100.00	100.00	100.00	100.00
Trace Elements (ppm)												
V	N.D.†	N.D.	N.D.	N.D.	N.D.	N.D.	N.D.	120	93	107	171	113
Cr	2720	N.D.	2790	2450	2550	N.D.	N.D.	2091	3813	2739	1944	3416
Co	N.D.	N.D.	N.D.	N.D.	N.D.	N.D.	N.D.	109	112	90	93	107
Ni	1260	N.D.	1120	1290	1140	N.D.	N.D.	N.D.	N.D.	N.D.	N.D.	N.D.
Zn	N.D.	N.D.	N.D.	N.D.	N.D.	N.D.	N.D.	90	69	71	88	145
Rb	4	N.D.	5	4	4	N.D.	N.D.	6	18	5	6	5
Sr	25	N.D.	8	7	22	N.D.	N.D.	19	11	25	13	15
Y	8	N.D.	3	2	6	N.D.	N.D.	6	6	7	13	4
Zr	27	N.D.	25	28	41	N.D.	N.D.	34	33	52	41	31
Nb	3	N.D.	3	4	4	N.D.	N.D.	4	7	4	4	3
CIPW Weight Norms												
Or	0.5	0.5	0.3	0.2	1.2	0.6	0.3	0.4	2.0	0.3	0.3	0.0
Ab	2.5	4.1	1.2	0.3	5.8	3.7	1.4	2.9	0.6	1.0	4.7	0.6
An	13.9	12.8	11.6	5.9	12.2	9.4	14.5	17.0	11.9	18.1	16.0	14.5
C	0.0	0.0	0.0	2.3	0.0	0.0	0.0	0.0	0.0	0.0	0.0	1.2
Di	9.8	5.6	7.0	0.0	9.3	8.0	10.5	4.7	3.7	5.8	5.9	0.0
Hy	17.0	56.3	23.2	61.0	46.7	60.6	33.7	53.3	26.3	40.3	51.0	67.4
Ol	54.8	19.7	56.9	30.4	23.8	16.8	39.9	21.2	55.0	33.6	21.3	15.8
Il	0.5	0.5	0.5	0.4	0.6	0.6	0.6	1.0	0.0	1.0	1.0	0.0
Ap	0.1	0.0	0.0	0.2	0.1	0.1	0.0	0.0	0.0	0.0	0.0	0.0

(continued)

variation of the Tobacco Root rocks cannot be explained by olivine fractionation (see below). The CaO/Al_2O_3 (weight percent ratio) values for komatiites are typically ~1.0 or higher, whereas the Tobacco Root meta-ultramafic rocks have CaO/Al_2O_3 values less than 1.0 (Fig. 7). REE data are also inconsistent with typical upper-mantle protoliths, such as Alpine-type peridotites and those found in typical ophiolites, which are LREE depleted. Moreover, the observed Mg numbers (74–84) are much lower than expected for mantle rocks (88–92).

To identify alternative protoliths, the covariation of elements or their oxides was explored. Weight percent ratios of TiO_2 to Zr, V, and CaO were all found to be nearly constant, in spite of large variations in the concentrations of the individual elements and the wide geographic distribution of the ultramafic rocks. The most convincing ratio is Zr/TiO_2, which is shown in Figure 12. We interpret this to mean that (1) the meta-ultramafic rocks distributed across the Tobacco Root Mountains have a common or related origin and (2) these elements were immobile or conserved in the processes that produced the observed variety of ultramafic rock compositions. We feel confident in these conclusions because our analyses, from several labs, are consistent and match those of Cummings and McCulloch (1992).

With conserved elements identified, it is possible to quantify the relative variations of other elements and to test hypotheses regarding the cause of those variations (Pearce, 1968; Stanley and Russell, 1989) by using one of the conserved elements to

TABLE 2. WHOLE-ROCK CHEMICAL ANALYSES OF META-ULTRAMAFIC ROCKS (*continued*)

Host	SPMS	SPMS	SPMS	SPMS	SPMS	SPMS	SPMS	ICMS	ICMS	PMMMS	PMMMS
12T	042140E	042146E	041704E	041546E	042116E	042060E	042056E	041671E	041663E	042419E	042776E
UTM	503997N	503994N	504553N	504658N	504020N	504041N	504041N	504011N	504011N	506470N	506277N
Sample	WAM-7f	WAM-7g	WAM-23a	WAM-26	WAM-27a	WAM-29a	WAM-29c	WAM-19a	WAM-19b	WAM-10a	WAM-14a
Oxide (wt%)											
SiO_2	45.94	49.40	53.92	52.56	49.67	46.06	52.05	48.68	46.24	47.51	46.62
TiO_2	0.26	0.38	0.23	0.29	0.31	0.30	0.23	0.36	0.37	0.29	0.20
Al_2O_3	5.34	7.79	4.37	4.54	7.17	7.20	5.47	7.31	8.24	5.99	5.66
FeO*	12.50	10.59	10.41	9.46	11.26	13.20	12.33	13.58	13.54	10.67	12.46
MnO	0.32	0.47	0.15	0.14	0.55	0.45	0.52	0.24	0.29	0.39	0.35
MgO	31.28	23.71	26.86	28.63	25.29	27.85	24.99	23.57	25.93	28.96	30.27
CaO	4.01	6.90	3.49	3.86	4.96	4.43	3.85	6.05	5.35	6.07	4.30
Na_2O	0.28	0.54	0.54	0.45	0.67	0.41	0.49	0.12	0.00	0.07	0.12
K_2O	0.02	0.14	0.01	0.04	0.07	0.05	0.04	0.05	0.00	0.01	0.00
P_2O_5	0.04	0.06	0.02	0.03	0.04	0.06	0.02	0.04	0.04	0.04	0.02
Total	100.00	100.00	100.00	100.00	100.00	100.00	100.00	100.00	100.00	100.00	100.00
Trace Elements (ppm)											
V	94	125	100	88	145	135	132	154	156	95	72
Cr	3174	1832	3631	4061	1970	3271	2828	1764	2688	3427	2596
Co	133	82	129	116	107	115	100	116	115	103	122
Ni	N.D.†	N.D.	N.D.	N.D.	N.D.	N.D.	N.D.	N.D.	N.D.	N.D.	N.D.
Zn	74	61	76	104	74	81	95	60	77	69	79
Rb	4	3	7	6	0	4	8	1	1	5	0
Sr	19	23	20	30	18	13	17	13	20	98	21
Y	3	12	6	8	14	6	0	8	10	6	2
Zr	30	35	35	44	35	36	26	33	38	41	24
Nb	3	5	5	8	2	2	2	4	5	3	2
CIPW Weight Norms											
Or	0.1	0.8	0.1	0.2	0.4	0.3	0.2	0.3	0.0	0.1	0.0
Ab	2.4	4.6	4.6	3.8	5.7	3.5	4.2	1.0	0.0	0.6	1.0
An	13.3	18.4	9.5	10.3	16.4	17.7	12.6	19.3	22.5	16.0	14.9
C	0.0	0.0	0.0	0.0	0.0	0.0	0.0	0.0	0.0	0.0	0.0
Di	5.1	12.4	6.2	6.9	6.4	3.2	5.1	8.5	3.1	11.1	5.0
Hy	27.8	37.7	69.9	60.6	43.3	29.3	63.0	46.3	37.0	33.7	34.0
Ol	50.8	25.2	9.4	17.5	27.2	45.4	14.4	23.9	36.7	38.0	44.6
Il	0.0	1.0	0.0	1.0	1.0	1.0	0.0	1.0	1.0	1.0	0.0
Ap	0.0	0.0	0.0	0.0	0.0	0.0	0.0	0.0	0.0	0.0	0.0

Note: Data from Polson (1994) and MacFarlane (1996b). MacFarlane data are normalized to 100% without loss on ignition (LOI). SPMS—Spuhler Peak Metamorphic Suite; ICMS—Indian Creek Metamorphic Suite; PMMMS—Pony–Middle Mountain Metamorphic Suite; UTM—Universal Transverse Mercator.

*FeO—total iron as FeO.

†N.D.—no data.

normalize the data. This must be done with caution because of statistical correlations introduced by using a common denominator on both axes (e.g., Rollinson and Roberts, 1986). Because these are ultramafic rocks, olivine fractionation is a logical mechanism to explore for compositional variation. If olivine fractionation is the principal cause of silica variation, then a plot of the molar ratio (MgO + FeO)/TiO_2 versus SiO_2/TiO_2 should yield a trend with a slope of two. As shown in Figure 13, the slope of the trend line is close to one, which would be expected for orthopyroxene fractionation. Plotting other combinations of oxides to look for plagioclase and for plagioclase + clinopyroxene fractionation (also on Fig. 13) indicates that there is little variation of CaO, Al_2O_3, or Na_2O relative to TiO_2.

It is clear from Figure 13 that the majority of the chemical variation of SiO_2 relative to a conserved TiO_2 is due to the removal or accumulation of one or more Mg-Fe silicates. With a slope near one, orthopyroxene is probably important. Additional tests, not involving Pearce element ratio diagrams,

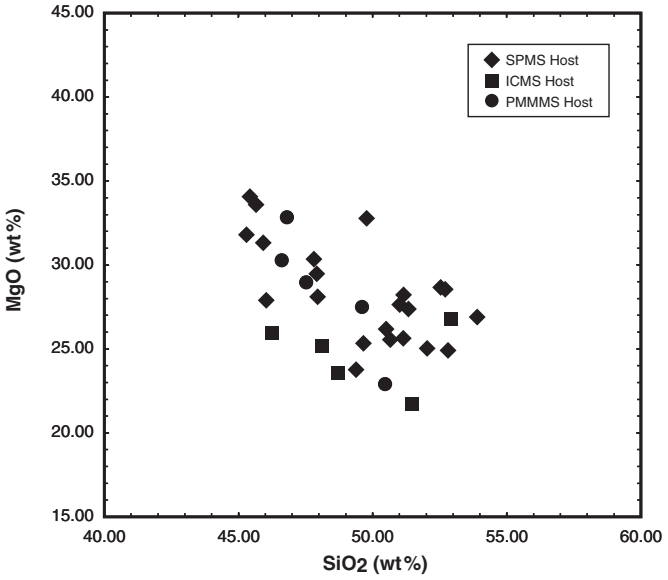

Figure 6. Variation diagram showing weight percent MgO vs. weight percent SiO_2. Different symbols are used for meta-ultramafic rocks that occur in different hosts. SPMS—Spuhler Peak Metamorphic Suite; ICMS—Indian Creek Metamorphic Suite; PMMMS—Pony–Middle Mountain Metamorphic Suite.

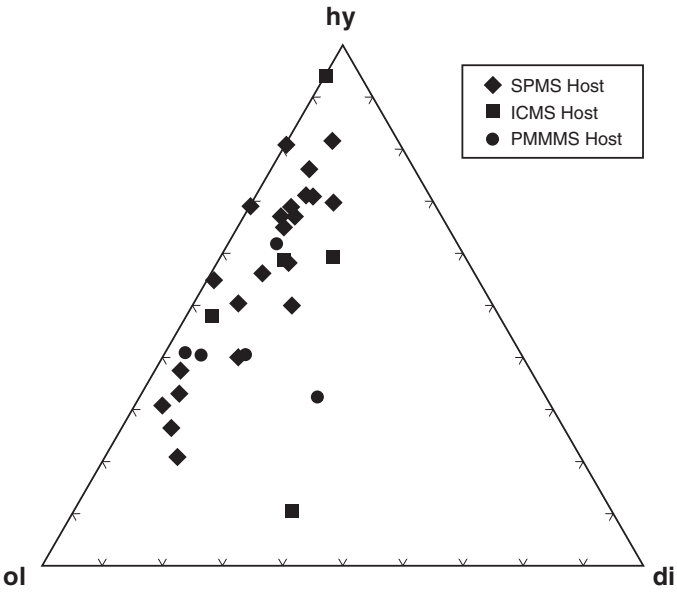

Figure 8. Meta-ultramafic rock chemical analyses are shown in terms of the relative proportions of the mafic CIPW weight norm minerals olivine (ol), hypersthene (hy), and diopside (di). The data are consistent with a protolith rich in orthopyroxene and olivine with subordinate clinopyroxene (and plagioclase—see Table 2). SPMS—Spuhler Peak Metamorphic Suite; ICMS—Indian Creek Metamorphic Suite; PMMMS—Pony–Middle Mountain Metamorphic Suite.

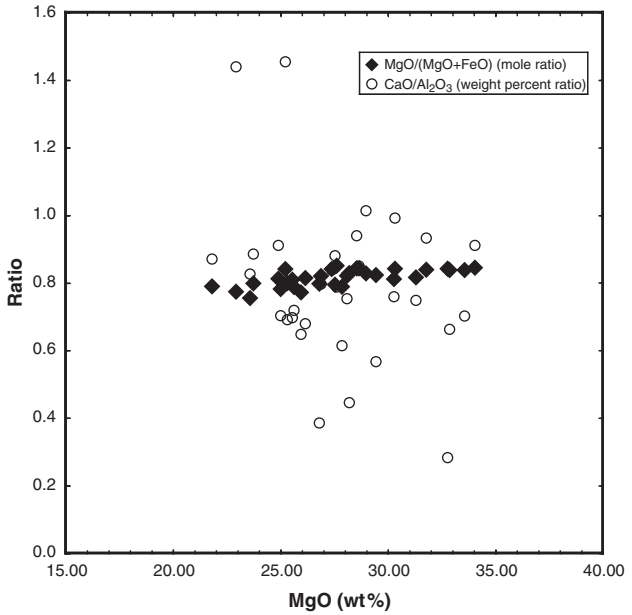

Figure 7. Variation diagram showing weight percent ratio CaO/Al_2O_3 vs. weight percent MgO and the mole ratio MgO/(MgO + FeO) vs. weight percent MgO.

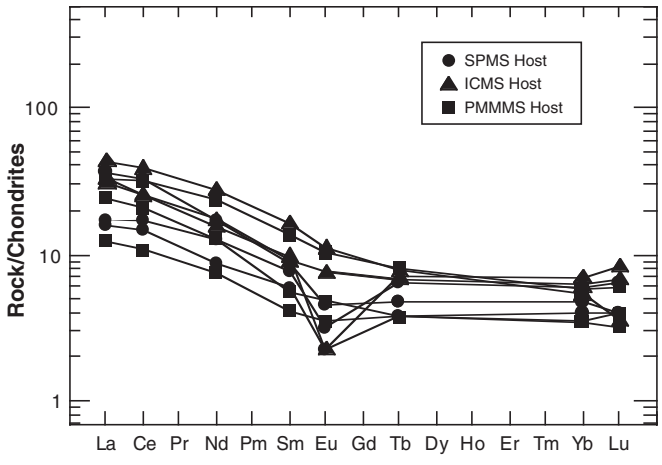

Figure 9. Rare earth data for the Tobacco Root meta-ultramafic rocks normalized to the chondrite values of Sun and McDonough (1989). All samples are enriched in the light rare earth elements and several show negative Eu anomalies. SPMS—Spuhler Peak Metamorphic Suite; ICMS—Indian Creek Metamorphic Suite; PMMMS—Pony–Middle Mountain Metamorphic Suite.

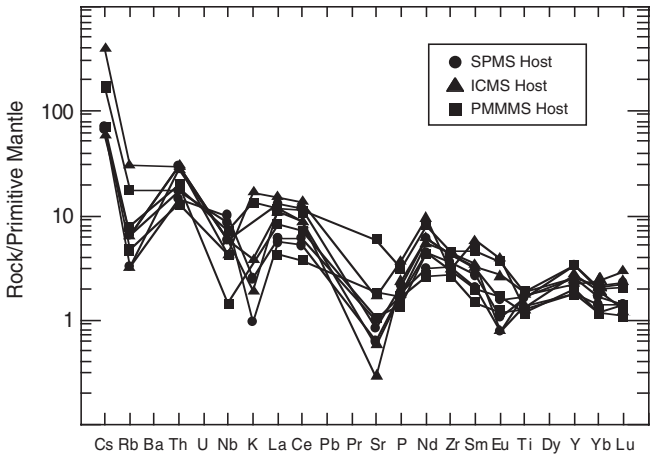

Figure 10. Trace element data for the Tobacco Root meta-ultramafic rocks normalized to the primitive mantle values of Sun and McDonough (1989). Note that several samples are depleted in K, Sr, or Eu and all are enriched in Cs. SPMS—Spuhler Peak Metamorphic Suite; ICMS—Indian Creek Metamorphic Suite; PMMMS—Pony–Middle Mountain Metamorphic Suite.

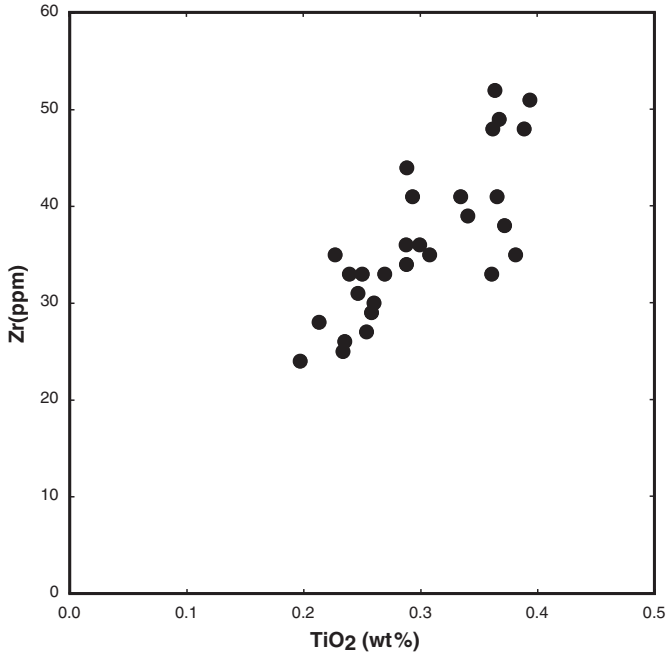

Figure 12. Variation of Zr (ppm) vs. TiO_2 (wt%) for analyzed Tobacco Root meta-ultramafic rocks. Although there is some scatter, the ratio of the concentrations of these two components is nearly constant. We interpret this to mean that both are incompatible with any fractionating phase.

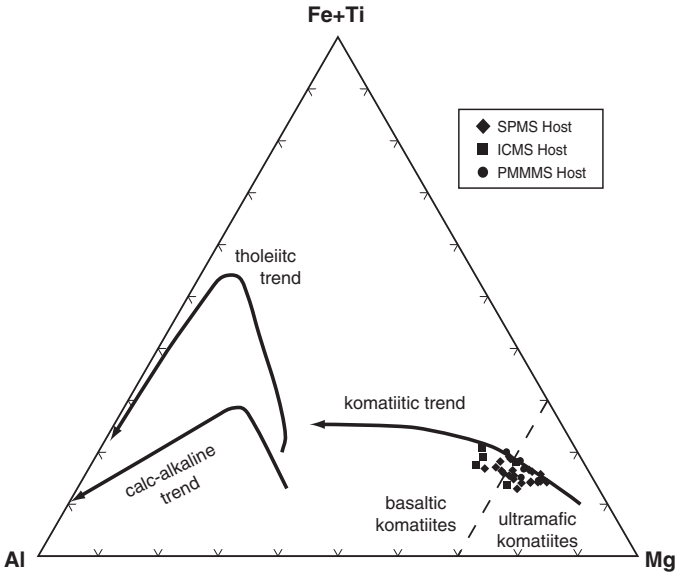

Figure 11. Meta-ultramafic rock chemical analyses are shown in terms of the relative cation proportions of Al, Fe + Ti, and Mg. Compositional fields for komatiites and fractional crystallization trends are those proposed by Jensen (1976). SPMS—Spuhler Peak Metamorphic Suite; ICMS—Indian Creek Metamorphic Suite; PMMMS—Pony–Middle Mountain Metamorphic Suite.

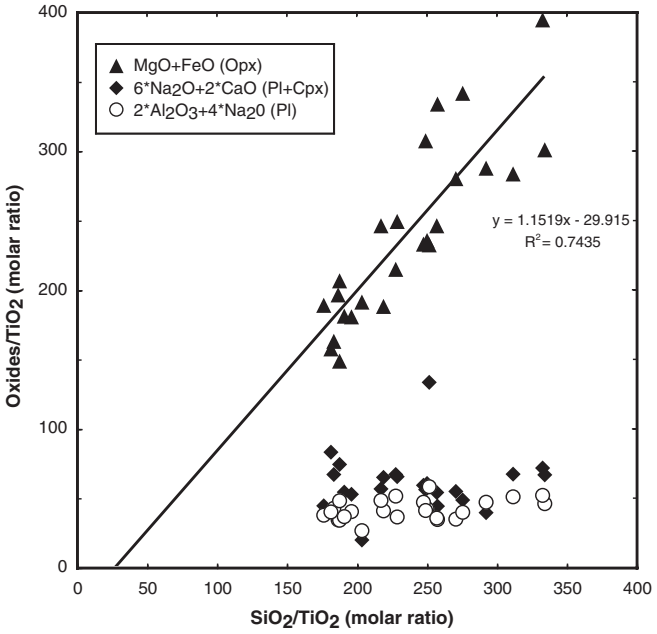

Figure 13. A variation diagram showing combinations of oxides in mole units vs. molar SiO_2, all divided by molar TiO_2. Combinations of elements chosen were selected to test for possible fractional crystallization of the minerals listed in parentheses. Both SiO_2 and FeO + MgO vary by a factor of two relative to TiO_2, whereas the quantities of CaO, Na_2O, and Al_2O_3 show little variation relative to TiO_2. Therefore, removal or addition of one or more Mg-Fe-rich, Ca-Al-poor minerals must be responsible for the chemical variation shown. If this mineral were olivine, the slope of the trend should be two. The observed slope (1.15) indicates that most of the variation is due to orthopyroxene addition or subtraction. Opx—orthopyroxene; Pl—plagioclase; Cpx—clinopyroxene.

support this conclusion. Figure 14 shows the meta-ultramafic rock compositions on a molar MgO + FeO, SiO_2, CaO + Al_2O_3 diagram. It is evident from this diagram that these rocks contain substantial amounts of normative orthopyroxene (see also Fig. 8). Indeed, we conclude that the protoliths of the Tobacco Root meta-ultramafic rocks were cumulates rich in orthopyroxene, which was also the preferred interpretation of Tendall (1978) based on modal data. Bulk compositions are appropriate for an orthopyroxene + olivine cumulate with intercumulus basaltic liquid (Fig. 14). Minor and trace element data are also consistent with orthopyroxene addition or subtraction as the major source of chemical variation. In the file of distribution coefficients for low-calcium pyroxene compiled by Roger Nielson for the GERM Kd Database (http://earthref.org/databases/KDD/index.html), only Cr, Ni, Sc, Co, and Zn (of the elements analyzed) have Kd values greater than one. For the Tobacco Root meta-ultramafic rocks, each of these elements varies in the manner expected for compatible elements: (1) Their ratios relative to TiO_2 decrease as SiO_2/TiO_2 decreases. (2) Their weight percentage decreases as the weight percentage of MgO decreases (see Figs. 15 and 16). Other trace elements, notably V, Y, and Zr, show incompatible trends.

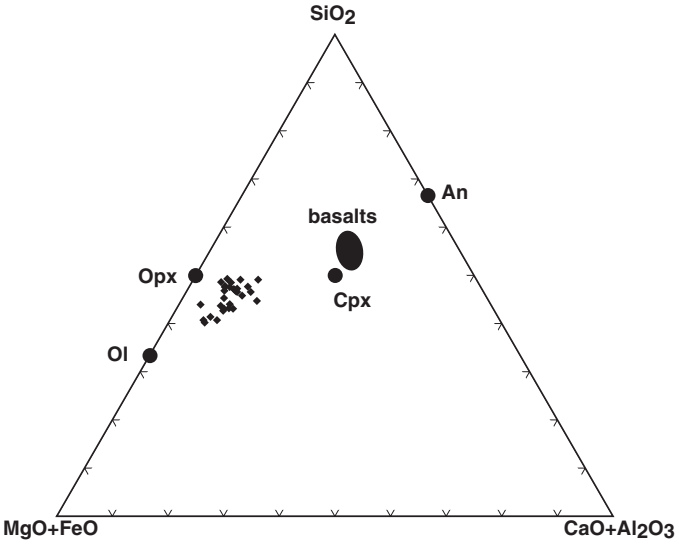

Figure 14. Meta-ultramafic rock chemical analyses are shown in terms of the relative mole proportions of MgO + FeO, SiO_2, and CaO + Al_2O_3. Compositions of olivine (Ol), orthopyroxene (Opx), clinopyroxene (Cpx), anorthite (An), and typical basalts are shown for reference.

DISCUSSION

The geochemistry of the Tobacco Root meta-ultramafic rocks has significant implications regarding their origin and tectonic setting. Low Mg numbers and LREE enrichment are inconsistent with an upper-mantle origin. Major and trace element data match the patterns expected for orthopyroxene-rich cumulates. Such rocks occur in oceanic settings, but orthopyroxene is generally subordinate to olivine and clinopyroxene, and the rocks are not LREE enriched (e.g., Meyer et al., 1989; Ross and Elthon, 1993). Orthopyroxene cumulates occur in suprasubduction zone ophiolites (Pearce et al., 1984), but the geochemical characteristics of the suprasubduction zone ophiolites, such as the typical TiO_2 values (<0.05 wt%), are not good matches with the Tobacco Root data (TiO_2 of 0.2–0.4 wt%). Abundant orthopyroxene is more typical of the crystallization of a continental tholeiite, such as the Stillwater igneous complex, than an oceanic tholeiite (Campbell, 1985). Campbell (1985) argued that additional silica assimilated by continental tholeiites directs the olivine fractionation path to cross the orthopyroxene reaction boundary, rather than to intersect the clinopyroxene cotectic (in the system olivine-clinopyroxene-silica) as in oceanic tholeiites. Elevated pressure shifts the olivine to orthopyroxene reaction curve away from silica on the same diagram, and also can lead to orthopyroxene fractionation. Some Archean, high-magnesium basalts show flat to light element–enriched REE patterns (Sun and Nesbitt, 1978; Sun, 1984) and silica enrichment, possibly reflecting an origin similar to the Tobacco Root rocks. Other Precambrian cumulate rocks from a continental setting also are rich in orthopyroxene (e.g., Srikantappa et al., 1984).

Continental tholeiites commonly occur in rift settings where fractional crystallization can lead to mafic rocks that match the

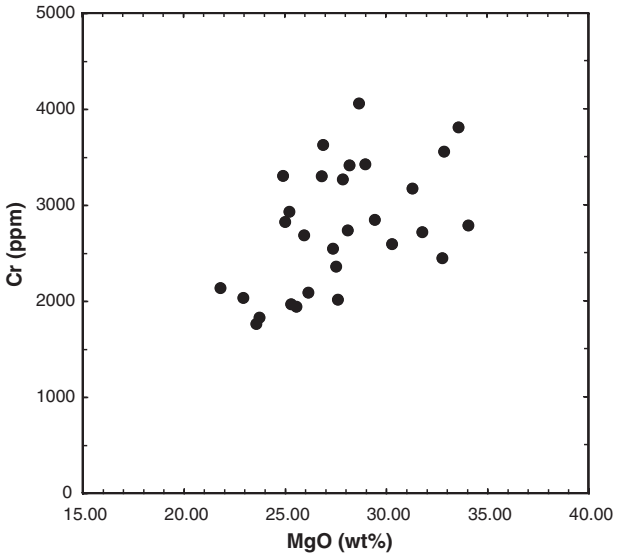

Figure 15. Variation diagram showing ppm Cr vs. weight percent MgO. Cr increases as MgO increases, which is consistent with the accumulation of orthopyroxene in which Cr is concentrated.

geochemistry of the Tobacco Root meta-ultramafic rocks (Crawford et al., 1984). Interestingly, the 2.06 Ga metamorphosed mafic dikes and sills (MMDS) that occur in the Tobacco Root Mountains are believed to have been intruded in a rift setting and sample a magma source that has undergone considerable fractional crystallization of orthopyroxene, as well as clinopyroxene

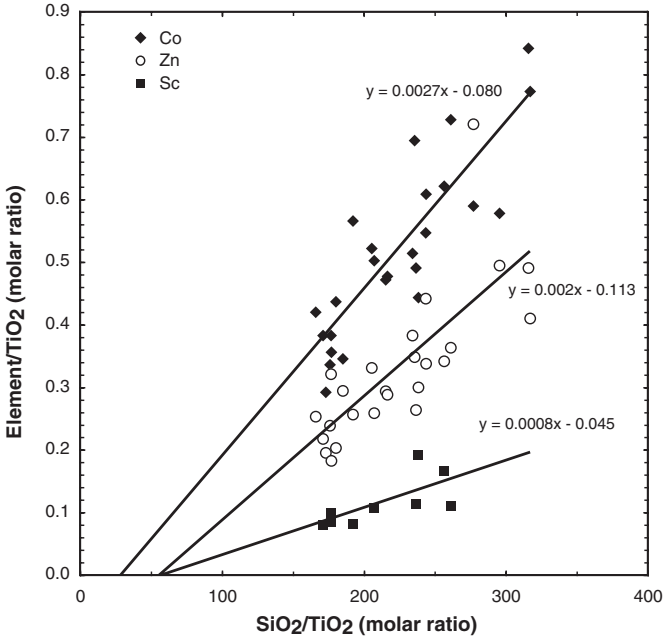

Figure 16. A variation diagram showing elements in mole units vs. molar SiO_2, all divided by molar TiO_2. Each of these elements is compatible with orthopyroxene and each ratio increases as SiO_2/TiO_2 increases, consistent with the accumulation of orthopyroxene.

and plagioclase (Brady et al., 2004, this volume, Chapter 5). Thus, it is possible that the MMDS and the meta-ultramafic rocks are related through the process of fractional crystallization. Both rock groups have similar light element–enriched REE patterns, with the MMDS values higher on average by a factor of four or more. Many of the ultramafic bodies occur in the Spuhler Peak Metamorphic Suite, which contains a significant volume of mafic rocks. However, the REE values for the Spuhler Peak Metamorphic Suite mafic rocks are similar in magnitude to the meta-ultramafic REE values (~10× chondrite), but with flat or LREE-depleted patterns (Burger et al., 2004, this volume, Chapter 3). So the only local candidate likely related by fractionation to the meta-ultramafic rock magmatic suite appears to be the MMDS. Cordua (1973) suggested that the MMDS and meta-ultramafic rocks might be related because they commonly occur near one another in the Tobacco Root Mountains. However, we believe that any current juxtaposition is tectonic and not directly related to the possibility of a common origin.

Meta-ultramafic rocks occur as isolated, podiform bodies in all three major Precambrian rock suites of the Tobacco Root Mountains. Based on the geochemical evidence for a common or related origin and on other descriptive data presented in this paper, we conclude that these bodies were tectonically emplaced rather than being small ultramafic intrusions. Elsewhere in this volume (Brady et al., 2004, this volume, Chapter 5), it is demonstrated that the Spuhler Peak Metamorphic Suite was not present for the 2.45 Ga metamorphism of the Pony–Middle Mountain Metamorphic Suite and the Indian Creek Metamorphic Suite, or for the 2.06 Ga intrusion of the MMDS. Therefore, it appears that the current distribution of ultramafic rocks was accomplished during the Big Sky orogeny at 1.78–1.72 Ga, which was probably also responsible for the emplacement of the Spuhler Peak Metamorphic Suite. If both the meta-ultramafic rocks and the Spuhler Peak Metamorphic Suite were tectonically emplaced ca. 1.78 Ga, it makes sense that many of the meta-ultramafic bodies studied in the field were found in or near to the Spuhler Peak Metamorphic Suite. Perhaps future detailed structural work will be able to use the distribution of meta-ultramafic rocks to unravel more of the complex deformation that must have accompanied the Big Sky orogeny.

ACKNOWLEDGMENTS

We would like to thank the Keck Geology Consortium, its member colleges, and especially the W.M. Keck Foundation for providing support for this project. Additional funding to K.E. Johnson was provided by a Summer Faculty Fellowship from the University of New Orleans. Instrumental neutron activation analysis data were provided by Oregon State University under the Department of Energy's Reactor Sharing Program. Other members of the Tobacco Root Project for 1995–1996 who deserve special thanks for assistance in locating and sampling previously "uncharted" ultramafic rocks in all three metamorphic suites are Kathleen DeGraff, Heidi Mohlman, David Owen, Caroline Tuit, Jennifer Martin, Jillian Hirst, Wilfredo Chaparro, Steven Kranenburg, Jason Cox, and Karl Wegeman. We thank especially Gary Ernst and Edward Stoddard, who improved the manuscript with their timely and incisive reviews.

REFERENCES CITED

Arndt, N.T., and Nisbet, E.G., 1982, What is a komatiite?, *in* Arndt, N.T., and Nisbet, E.G., eds., Komatiites: London, George Allen and Unwin, p. 19–27.

Arndt, N.T., Naldrett, A.J., and Pyke, D.R., 1977, Komatiitic and iron-rich tholeiitic lavas of Munro Township, Northeast Ontario: Journal of Petrology, v. 18, p. 319–369.

Berman, R.G., 1988, Internally consistent thermodynamic data for minerals in the system Na_2O-K_2O-CaO-MgO-FeO-Fe_2O_3-Al_2O_3-SiO_2-TiO_2-H_2O-CO_2: Journal of Petrology, v. 29, no. 2, p. 445–522.

Brady, J.B., Mohlman, H.K., Harris, C., Carmichael, S.K., Jacob, L.K., and Chaparro, W.R., 2004, General geology and geochemistry of metamorphosed Proterozoic mafic dikes and sills, Tobacco Root Mountains, Montana, *in* Brady, J.B., et al., eds., Precambrian geology of the Tobacco Root Mountains, Montana: Boulder, Colorado, Geological Society of America Special Paper 377, p. 89–104 (this volume).

Burger, H.R., 1966, Structure, petrology, and economic geology of the Sheridan district, Madison County, Montana [Ph.D. thesis]: Bloomington, Indiana University, 156 p.

Burger, H.R., 1967, Bedrock geology of the Sheridan district, Madison County, Montana: Montana Bureau of Mines and Geology Memoir 41, 22 p.

Burger, H.R., 2004, General geology and tectonic setting of the Tobacco Root Mountains, Montana, *in* Brady, J.B., et al., eds., Precambrian geology of the Tobacco Root Mountains, Montana: Boulder, Colorado, Geological Society of America Special Paper 377, p. 1–14 (this volume).

Burger, H.R., Peck, W.H., Johnson, K.E., Tierney, K.A., Poulsen, C.J., Cady, P., Lowell, J., MacFarlane, W.A., Sincock, M.J., Archuleta, L.L., Pufall, A., and Cox, M.J., 2004, Geology and geochemistry of the Spuhler Peak

Metamorphic Suite, *in* Brady, J.B., et al., eds., Precambrian geology of the Tobacco Root Mountains, Montana: Boulder, Colorado, Geological Society of America Special Paper 377, p. 47–70 (this volume).

Campbell, J.H., 1985, The difference between oceanic and continental tholeiites; a fluid dynamic explanation: Contributions to Mineralogy and Petrology, v. 91, p. 37–43.

Cheney, J.T., Brady, J.B., Tierney, K.A., DeGraff, K.A., Mohlman, H.K., Frisch, J.D., Hatch, C.E., Steiner, M.L., Carmichael, S.K., Fisher, R.G.M., Tuit, C.B., Steffen, K.J., Cady, P., Lowell, J., Archuleta, L.L., Hirst, J., Wegmann, K.W., and Monteleone, B., 2004a, Proterozoic metamorphism of the Tobacco Root Mountains, Montana, *in* Brady, J.B., et al., eds., Precambrian geology of the Tobacco Root Mountains, Montana: Boulder, Colorado, Geological Society of America Special Paper 377, p. 105–129 (this volume).

Cheney, J.T., Webb, A.A.G., Coath, C.D., and McKeegan, K.D., 2004b, In situ ion microprobe $^{207}Pb/^{206}Pb$ dating of monazite from Precambrian metamorphic suites, Tobacco Root Mountains, Montana, *in* Brady, J.B., et al., eds., Precambrian geology of the Tobacco Root Mountains, Montana: Boulder, Colorado, Geological Society of America Special Paper 377, p. 151–179 (this volume).

Cordua, W.S., 1973, Precambrian geology of the southern Tobacco Root Mountains, Madison County, Montana [Ph.D. thesis]: Bloomington, Indiana University, 247 p.

Crawford, A.J., Cameron, W.E., and Keays, R.R., 1984, The association of boninite low-Ti andesite-tholeiite in the Heatcote Greenstone Belt, Victoria; ensimatic setting for the early Lachlan fold belt: Australian Journal of Earth Sciences, v. 31, p. 161–175.

Cummings, M.L., and McCulloch, W.R., 1992, Geochemistry and origin of amphibolite and ultramafic rocks, Branham Lakes area, Tobacco Root Mountains, southwestern Montana, *in* Bartholomew, M.J., et al., eds., Basement tectonics 8: Characterization and comparison of ancient and Mesozoic continental margins—Proceedings of the 8th International Conference on Basement Tectonics (Butte, Montana, 1988): Dordrecht, Netherlands, Kluwer Academic Publishers, p. 323–340.

Desmarais, N.R., 1981, Metamorphosed Precambrian ultramafic rocks in the Ruby Range, Montana: Precambrian Research, v. 16, p. 67–101.

Friberg, N., 1976, Petrology of a metamorphic sequence of upper amphibolite facies in the central Tobacco Root Mountains, southwestern Montana [Ph.D. thesis]: Bloomington, Indiana University, 146 p.

Garihan, J.M., 1979, Geology and structure of the central Ruby Range, Madison County, Montana: Geological Society of America Bulletin, v. 90, p. 323–326 (Part I), p. 695–788 (Part II).

Gillmeister, N.M., 1972, Petrology of Precambrian rocks in the central Tobacco Root Mountain, Madison County, Montana [Ph.D. thesis]: Cambridge, Massachusetts, Harvard University, 201 p.

Gillmeister, N.M., 1976, Garnet-bearing metamorphosed ultramafic rocks from southwestern Montana: Eos (Transactions, American Geophysical Union), v. 57, no. 4, p. 338.

Hanley, T.B., 1975, Structure and petrology of the northwestern Tobacco Root Mountains, Madison County, Montana [Ph.D. thesis]: Bloomington, Indiana University, 289 p.

Harms, T.A., Burger, H.R., Blednick, D.G., Cooper, J.M., King, J.T., Owen, D.R., Lowell, J., Sincock, M.J., Kranenburg, S.R., Pufall, A., and Picornell, C.M., 2004, Character and origin of Precambrian fabrics and structures in the Tobacco Root Mountains, Montana, *in* Brady, J.B., et al., eds., Precambrian geology of the Tobacco Root Mountains, Montana: Boulder, Colorado, Geological Society of America Special Paper 377, p. 203–226 (this volume).

Heinrich, E.W., 1963, Paragenesis of clinohumite and associated minerals from Wolf Creek, Montana: American Mineralogist, v. 48, p. 597–613.

Hess, D.F., 1967, Geology of pre-Beltian rocks in the central and southern Tobacco Root Mountains (Montana), with reference to superposed effects of the Laramide age Tobacco Root Batholith [Ph.D. thesis]: Bloomington, Indiana University, 333 p.

Hess, P.C., 1989, Origins of igneous rocks: Cambridge, Massachusetts, Harvard University Press, 336 p.

Holland, T.J.B., and Powell, R., 1998, An internally consistent thermodynamic data set for phases of petrological interest: Journal of Metamorphic Geology, v. 16, no. 3, p. 309–343.

Jahn, B.M., and Zhang, Z.Q., 1984, Radiometric ages (Rb-Sr, Sm-Nd, U-Pb) and REE geochemistry of Archean granulite gneisses from Eastern Hebei Province, China, *in* Kroner, A., et al., eds., Archean geochemistry: Berlin, Springer Verlag, p. 205–230.

Jensen, L.S., 1976, A new cation plot for classifying subalkalic volcanic rocks: Ontario Geological Survey Miscellaneous Paper 66, 22 p.

Johnson, K.E., Burger, H.R., Brady, J.B., Cheney, J.T., Harms, T.A., Thomas, R.B., and MacFarlane, W.A., 1996, Archean meta-ultramafics in the Tobacco Root Mountains, SW Montana: An evaluation of the metamorphic history and protolith: Geological Society of America Abstracts with Programs, v. 28, no. 7, p. 493.

Kalsbeek, F., and Manatschal, G., 1999, Geochemistry and tectonic significance of peridotitic and metakomatiitic rocks from the Ussuit area, Nagssugtoqidian orogen, West Greenland: Precambrian Research, v. 94, p. 101–120.

MacFarlane, W.A., 1996a, A Geochemical and petrographic analysis of the meta-ultramafic rocks in the Tobacco Root Mountains, southwest Montana, *in* Mendelson, C.V., and Mankiewicz, C., eds., Ninth Keck research symposium in geology: Williamstown, Massachusetts, Williams College, p. 106–109.

MacFarlane, W.A., 1996b, A geochemical and petrographic analysis of the meta-ultramafic rocks in the Tobacco Root Mountains, southwest Montana [B.A. thesis]: Colorado Springs, Colorado College, 132 p.

Merrill, G.P., 1895, Notes on some eruptive rocks from Gallatin, Jefferson, and Madison counties, Montana: Proceedings of the United States National Museum, p. 637–673.

Meyer, P.S., Dick, H.J.B., and Thompson, G., 1989, Cumulate gabbros from the southwest Indian Ridge, 54° S, 7°16′ E: Implications for magmatic processes at a slow spreading ridge: Contributions to Mineralogy and Petrology, v. 103, p. 44–63.

Mueller, P.A., Burger, H.R., Wooden, J.L., Heatherington, A.L., Mogk, D.W., and D'Arcy, K., 2004, Age and evolution of the Precambrian crust of the Tobacco Root Mountains, Montana, *in* Brady, J.B., et al., eds., Precambrian geology of the Tobacco Root Mountains, Montana: Boulder, Colorado, Geological Society of America Special Paper 377, p. 181–202 (this volume).

Occhipinti, S.A., Swager, C.P., and Pirajno, F., 1998, Structural-metamorphic evolution of the Paleoproterozoic Bryah and Padbury Groups during the Capricorn orogeny, Western Australia: Precambrian Research, v. 90, p. 141–158.

Paktunc, A.D., 1984, Metamorphism of the ultramafic rocks of the Thompson Mine, Thompson Nickel Belt, northern Manitoba: Canadian Mineralogist, v. 22, p. 77–91.

Pearce, J.A., Lippard, S.J., and Roberts, S., 1984, Characteristics and tectonic significance of supra-subduction zone ophiolites, *in* Kokelaar, B.P., and Howells, M.F., eds., Marginal basin geology; volcanic and associated sedimentary and tectonic processes in modern and ancient marginal basins: Geological Society [London] Special Publication 16, p. 74–94.

Pearce, T.H., 1968, A contribution to the theory of variation diagrams: Contributions to Mineralogy and Petrology, v. 19, p. 142–157.

Poulsen, C.J., 1994, Origin, metamorphic history, and tectonic setting of Archean rocks from the Spuhler Peak Assemblage, Tobacco Root Mountains, Montana [B.A. thesis]: Northfield, Minnesota, Carleton College, 54 p.

Reid, R.R., 1963, Metamorphic rocks of the northern Tobacco Root Mountains, Madison County, Montana: Geological Society of America Bulletin, v. 74, p. 293–305.

Rollinson, H.R., and Roberts, C.R., 1986, Ratio correlations and major element mobility in altered basalts and komatiites: Contributions to Mineralogy and Petrology, v. 93, p. 89–97.

Root, F.K., 1965, Structure, petrology, and mineralogy of pre-Beltian metamorphic rocks of the Pony-Sappington area, Madison County, Montana [Ph.D. thesis]: Bloomington, Indiana University, 184 p.

Rosing, M.T., and Rose, N.M., 1993, The role of ultramafic rocks in regulating the concentrations of volatile and nonvolatile components during deep crustal metamorphism: Chemical Geology, v. 108, p. 187–200.

Ross, K., and Elthon, D., 1993, Cumulates from strongly depleted mid-ocean-ridge basalt: Nature, v. 365, p. 826–829.

Sanford, R.F., 1982, Growth of ultramafic reaction zones in greenschist to amphibolite facies metamorphism: American Journal of Science, v. 282, p. 543–616.

Schmädicke, E., 2000, Phase relations in peridotitic and pyroxenitic rocks in the model systems CMASH and NCMASH: Journal of Petrology, v. 41, p. 69–86.

Sincock, M.J., 1994, Structural and metamorphic history of an intensely deformed zone, lower Branham Lake, southern Tobacco Root Mountains, Montana [B.A. thesis]: Lancaster, Pennsylvania, Franklin and Marshall College, 31 p.

Spear, F.S., 1993, Metamorphic phase equilibria and pressure-temperature-time paths, Mineralogical Society of America Monographs: Washington, D.C., Mineralogical Society of America, 799 p.

Srikantappa, C., Hormann, P.K., and Raith, M., 1984, Petrology and geochemistry of layered ultramafic to mafic complexes from the Archean craton of Karnataka, southern India, *in* Kroner, A., et al., eds., Archean geochemistry: Berlin, Springer Verlag, p. 138–160.

Stanley, C.R., and Russell, J.K., 1989, Petrologic hypothesis testing with Pearce element ratio diagrams; derivation of diagram axes: Contributions to Mineralogy and Petrology, v. 103, p. 78–89.

Sun, S.S., 1984, Geochemical characteristics of Archaean ultramafic and mafic volcanic rocks; implications for mantle composition and evolution, *in* Kroener, A., et al., eds., Archaean geochemistry: The origin and evolution of the Archaean continental crust: Berlin, Springer Verlag, p. 25–46.

Sun, S.S., and McDonough, W.F., 1989, Chemical and isotopic systematics of oceanic basalts; implications for mantle composition and processes, *in* Saunders, A.D., and Norry, M.J., eds., Magmatism in the ocean basins: Geological Society [London] Special Publication 42, p. 313–345.

Sun, S.S., and Nesbitt, R.W., 1978, Petrogenesis of Archaean ultrabasic and basic volcanics; evidence from rare earth elements: Contributions to Mineralogy and Petrology, v. 65, p. 301–325.

Tendall, B.A., 1978, Mineralogy and petrology of Precambrian ultramafic bodies from the Tobacco Root Mountains, Madison County, Montana [M.S. thesis]: Bloomington, Indiana University, 127 p.

Thomas, R.B., 1996a, Metamorphic history of Archean ultramafic pods in the Tobacco Root Mountains, southwestern Montana, *in* Mendelson, C.V., and Mankiewicz, C., eds., Ninth Keck research symposium in geology: Williamstown, Massachusetts, Williams College, p. 82–85.

Thomas, R.B., 1996b, Metamorphic history of Archean ultramafic pods of the Tobacco Root Mountains, southwestern Montana [B.A. thesis]: Williamstown, Massachusetts, Williams College, 125 p.

Vitaliano, C.J., Burger, H.R., Cordua, W.S., Hanley, T.B., Hess, D.P., and Root, F.K., 1979, Explanatory text to accompany geologic map of southern Tobacco Root Mountains, Madison County, Montana: Geological Society of America Map and Chart Series MC31, scale 1:62,500, 1 sheet, 8 p. text.

Wilson, M.L., and Hyndman, D.W., 1990, Tectonic interpretation of an Archean lithologic package enclosing iron-formation in the southern Tobacco Root and northern Ruby Ranges of southwestern Montana, USA, *in* Chauvel, J.J., ed., Ancient banded iron formations; regional presentations: Athens, Greece, Theophrastus Publishing, p. 27–61.

Wyllie, P.J., 1967, Ultramafic and ultrabasic rocks, *in* Wyllie, P.J., ed., Ultramafic and related rocks: New York and London, John Wiley & Sons, p. 1–7.

Manuscript Accepted by the Society September 12, 2003

Printed in the USA